New Delhi, 1995.

IMPACT OF CHANGES IN SURFACE ROUGHNESS ON SURFACE LAYER WINDS, TURBULENCE AND PLUME DISPERSION

G.Wu[1] and R.N. Meroney[2]

1. Senior Environmental Scientist, R.W. Beck, Denver, CO 80202-2615, USA

2. Professor of Civil Engineering, Colorado State University, Fort Collins, CO 80523, USA

Abstract

A wind-tunnel simulation of air flow over a step change of surface roughness at a scale ratio of 1:500 was conducted in the Meteorological Wind Tunnel (MWT) at Colorado State University. Measurements of mean velocity, turbulence and concentration distribution examined the response of the flow to changes from smooth-to-rough and rough-to-smooth transitions. Three different surface conditions of smooth, rough and very rough ($(z_o)_p$ = 7.5, 135 and 1,150 mm respectively) were examined in four combinations. Separate internal boundary layer depths were defined based on mean velocity, turbulent intensity and shear stress profiles. Dispersion processes outside of the internal boundary layer were dominated by the upstream flow characteristics. Dispersion from short stacks released near the transition region occurred at rates midway between those expected for the up- and down-wind surface conditions. Several first-order turbulence closure schemes and their associated assumptions were compared to the wind-tunnel data.

1.0 INTRODUCTION

Although the air flow over homogenous terrain has been extensively studied, air flow over a complex surface condition with abrupt changes in roughness and temperature occurs more often in nature. Indeed, it is extremely difficult to find perfectly homogeneous surface conditions on the Earth's surface. Atmospheric flow is strongly influenced by such surface conditions, and surface roughness changes can induce increases or decreases in relative turbulent mixing, change evaporation rates, cause entrainment of surface debris or dusts, influence the effectiveness of wind energy turbines, and increase or decrease shelter on buildings during hazardous wind events.

Air flow over inhomogeneous surfaces has been examined through atmospheric field observation, numerical simulation and wind-tunnel modeling. A review of previous research (Wu, 1992) revealed several unresolved questions about the behavior of air flow over surface inhomogeneities. A study was designed to illuminate a number of characteristics of flows influenced by changes in surface roughness, including a) permissible approximations for numerical or analytic models of the flow, b) the influence of "large" changes in surface roughness as opposed to the small perturbations previously reported, and c) behavior of 3-D turbulence structures induced by 2-D changes in roughness.

Measurements of wind field (mean velocity, turbulence structure) and plume dispersion were performed over seven test configurations including smooth, rough and very rough homogeneous surfaces, and four other combinations of smooth, rough and very rough surface texture. This paper describes the tests arrangement and instrumentation and discusses the implications of the test data.

2.0 NATURE OF AIR FLOW OVER A STEP CHANGE OF SURFACE ROUGHNESS

When air flows over inhomogeneous surface roughness, the flow may encounter a sudden or gradual change in roughness. The perturbed flow field can be divided into three regions in the horizontal direction as shown in Figure 1.0 A boundary layer will develop over the upwind surface (region I) that is in equilibrium with the underlying roughness. When this air flows over the neighboring region (region II), the bottom of the boundary layer will be modified by the new surface features. In region II, the flow field can be divided into three vertical layers. The velocity profiles, friction velocities and turbulence structures are all modified in the lower part of the atmospheric surface layer. The modified layer will increase in height with distance downwind of the roughness discontinuity. Above this modified layer the flow field continues to behave as it did over the upwind surface. This modified layer is called an internal boundary layer (IBL).

An equilibrium layer may be observed in the lower part of the IBL. The velocity profile and turbulence quantities inside this layer have adjusted to the new surface roughness conditions. The region between the equilibrium layer and the internal boundary layer is called the transition layer. The velocity and turbulence quantities inside this layer are transitional between the new equilibrium state (downstream surface conditions) and the old equilibrium state (upstream surface conditions). When the air flow travels sufficiently far downstream from the point of discontinuity, a new equilibrium will be reached with new surface forcing throughout the entire boundary layer (region III).

2.1 Analytic Models for Roughness Change Flows

When air flows over a step change in surface roughness, the mean flow accelerates or decelerates depending on whether the flow travels from a rough to a smooth surface or a smooth to rough surface. Predictions of the perturbations produced by surface roughness variations include the Karman-Pohlhausen integral methods (Elliott, 1958; Panofsky and Townsend, 1964; Taylor, 1967); similarity methods (Townsend, 1965a, 1965b); and linear-perturbation models (Jackson and Hunt, 1975; Walmsley et al., 1986).

The integral methods assume the flow is two dimensional, upstream flow is in turbulent equilibrium, air flow in region II within the IBL immediately adjusts to the new surface, and various distributions of vertical shear stress. The mean velocity profiles predicted downstream of the roughness discontinuity by such methods do not differ significantly. Similarity models postulate the flow is self-preserving such that the vertical profiles have the same form at all distances from the point of transition differing only in scales of velocity and length. The similarity models require a mixing length turbulence model which presumes that turbulence is in local equilibrium. The linear perturbation models argue that the flow is divided into two layers: (i) an inner layer of height ℓ in which shear stress has a significant effect on the flow and all roughness perturbations occur, and (ii) an outer region in which roughness effects are insignificant. The linear models permit specific formulations for the mean velocity and shear stress distribution; however, they are not appropriate for nonlinear perturbations or nonlinear synergism of two or more effects combined.

2.2 Numerical Models for Roughness Change Flows

A number of numerical calculations have been prepared to evaluate two-dimensional step change of surface roughness situations (see Wu, 1992, for complete summary) . The methods differ primarily in the form of the turbulence closure scheme chosen to solve the equations of motion: first, one-and-a-half, and second order. Since most of the closure schemes used are valid only in horizontal homogenous flow conditions, mean velocity and turbulence quantities were measured to verify whether the roughness change situation was suitable for such assumptions.

3.0 WIND-TUNNEL SIMULATION OF ATMOSPHERIC BOUNDARY LAYER AND DISPERSION PROCESSES

Similarity criteria pertinent to the physical simulation of atmospheric flow and dispersion over inhomogeneous surfaces are thoroughly summarized by Cermak (1975), Snyder (1982), and Meroney (1985, 1990). Wu (1992) determined that the present study required the following constraints to represent atmospheric flows,

a. $Re_* = u_* z_o/\nu > 1\text{-}5$; b. $(W_s/U)_p = (W_s/U)_m$;
c. $(\rho_s/\rho_a)_p = (\rho_s/\rho_a)_m$; d. $Re_s = W_s D/\nu_s > 300$;
e. Similar mean velocity profiles upstream; and
f. Similar turbulence profiles upstream;

where subscript m and p reflect model and prototype conditions respectively, and s and a prescribe stack and atmospheric properties. Such criteria assure that the model experiments are Reynolds number independent. The effects of Coriolis accelerations, thermal stratification, compressibility and dissipation are presumed to be trivial.

In the current experiments the turbulent Reynolds number, Re_*, equaled 3, 54, and 460 for the smooth, rough and very rough conditions, respectively; the stack Reynolds number, Re_s, was about 2,000 (a turbulence promoting ring was also installed inside the model stacks near the exit); and equilibrium turbulence profiles existed upwind of the surface roughness discontinuities. During the dispersion experiments a neutrally balanced methane mixture gas was released from the stacks, $(\rho_s/\rho_a) = 1$, with an effluent-to-stack height velocity ratio of $W_s/U = 1.5$. No stack downwash was noted, but a slight plume rise was observed due to momentum.

4.0 DATA ACQUISITION AND IMAGE ANALYSIS

All tests were performed in the Meteorological Wind Tunnel (MWT) of the Fluid Dynamics and Dispersion Laboratory, Colorado State University. The MWT is a closed-circuit wind tunnel with a test section 29.3 m long and 2 x 2 m in cross-section. Four evenly spaced 91 cm tall spires were placed across the tunnel entrance to initialize the simulated atmospheric boundary layer. The location of the origin of coordinates and any change in surface roughness occurred 21 m downwind of the entrance spires. The ceiling of the wind tunnel was adjusted to produce a zero pressure gradient in the mean flow direction.

Seven surface cases were examined (See Table 1), which included three homogeneous cases of a smooth tunnel floor, an array of 1.6 cm high twisted link chain elements placed 4 cm apart in rows perpendicular to the flow direction, and an array of 3.5 cm high twisted link chain elements similarly arranged. Four discontinuity situations were studied by combining smooth-rough, rough-smooth, smooth-very-rough, and very-rough-smooth sequences.

4.1 Instrumentation

Single and cross-hot-film anemometer measurements were used to document the flow structure over the various wall surface cases. Given accumulative effects of calibrator errors, calibration curve, and temperature correction errors the longitudinal, lateral and vertical instantaneous velocity measurements are accurate within ±10%, ±20% and ±20%, respectively. Concentration measurements were performed using a flame-ionization-detector gas chromatograph system. The gas sampling system obtained 50 integrated samples simultaneously, such that given joint influence of source gas, calibration, and sample extraction the normalized concentrations measured were accurate to within ±10%.

4.2 Image Analysis System

A visible smoke plume was produced by passing the simulant gas through a smoke generator. The visualization was recorded by a high-resolution television system on VCR tape. Subsequently, the images were analyzed by a digital video image processing system, and analysis of pixel densities identified instantaneous and time average plume centerline locations, vertical plume widths, and peak-to-mean concentration distributions (Wu, Higuchi, and Meroney; 1991).

5.0 CHARACTERISTICS OF FLOW OVER HOMOGENEOUS SURFACE ROUGHNESS

The simulated atmospheric boundary layer which developed during Cases 1, 2, and 3 is believed to match those of a full-scale flow scaled by 1:500. When power-law exponents, surface friction, longitudinal turbulent intensity and vertical intensity profiles were compared with average atmospheric characteristics tabulated by Counihan (1975) deviations ranged from 1 to 30% as shown in Table 2. Note that these deviations are from field data averaged over a wide range of measurement conditions, and the deviations need not be significant since such variations also exist among field studies.

Comparison of measured plume standard deviations, σ_y and σ_z, against formulae recommended by Briggs (1973) suggests that Case 1 and 2 produce plumes which disperse like those emitted in C-D stability over open country conditions and Case 3 produces plumes like those seen during D-E stability over urban conditions.

6.0 FLOW OVER A STEP CHANGE OF SURFACE ROUGHNESS

6.1 Mean Velocity and Friction Velocity Structure

After the discontinuity in surface roughness at coordinate location X = 0 cm, an internal boundary layer grows downward that contains beneath it the effect of change of roughness on mean velocities and turbulence structure (see Figures 2 through 5). As noted in Figure 4 for Case 6 (Smooth to very rough transition), the velocity profile approaches the homogeneous profile in the lower region as the flow moves downwind. Note the growth of the internal boundary layer (IBL) as the distance downwind increases.

Friction velocities, u_*, were calculated from the slope of the semilogarithmic velocity plots for data beneath $Z = 0.10\ \delta$. The friction velocity reacts abruptly to a change of roughness, either overshooting (smooth-to-rough) or undershooting (rough-to-smooth) the new equilibrium value. For air flow over rough-to-smooth the data scatters more than the smooth-to-rough situation. Perhaps upstream large eddies are transferred by advection downstream and destroy the local equilibrium conditions for greater distances.

6.2 Turbulent Kinetic Energy and Turbulent Shear Stress Structure

For smooth-to-rough transitions the turbulent kinetic energies increase above the downstream surface, whereas for the rough-to-smooth transitions the turbulent kinetic energies decrease. Larger changes occur for longitudinal and vertical velocities, whereas deviations of lateral turbulence intensity are small. Changes in longitudinal, lateral and vertical turbulence intensity profiles are displayed in Figure 6 for typical Case 6. Turbulent shear stresses are strongly distorted from their upstream equilibrium values near the transition area. The variations are not linear as postulated by Panofsky and Towsend (1964).

6.3 Scaling Function for Dimensionless Shear Stress

In an equilibrium flow momentum flux, mean shear and turbulent kinetic energy obey the following scaling rules:

$$\frac{\kappa z}{-\overline{uw}^{0.5}}\frac{\partial U}{\partial z} = \varphi = 1, \qquad \frac{-\overline{uw}}{c_0^2 E} = \alpha = 1 \tag{1}$$

$$where\ E = \overline{u^2} + \overline{v^2} + \overline{w^2}$$

Both ϕ and α deviate from their equilibrium values near the transition region. For decelerating flows (smooth-to-rough) ϕ and α exceed unity, and conversely, for accelerating flows (rough-to-smooth) ϕ and α are smaller than unity. Thus, for inhomogeneous conditions the turbulent shear stress does not relate to wind shear in the same manner as equilibrium flows.

6.4 Development of the Internal Boundary Layer

Detailed measurement of mean velocity, turbulent intensity, and shear stress profiles means that one can define the internal boundary layer depths based on each property of the flow. Although mean velocity and turbulent intensity define consistent internal boundary and equilibrium layer depths, the shear stress consistently penetrates further upward as shown in Figures 7 and 8 for Case 4 and Case 6, respectively..

6.5 Dispersion Processes over a Step Change of Surface Roughness

Dispersion measurements over the step changes of surface roughness indicate that the effects of the roughness change are only significant for low stack height releases (See typical Figure 9 for Cases 1, 3 and 6). Inside the internal boundary the concentration data for short stacks fall initially between the upstream control case and downstream control case values, but the data tends to approach the values of the upstream control case. Outside of the internal boundary layer the dispersion processes are dominated by the upstream flow characteristics. For high stack releases the upstream mean velocity and large turbulent eddies determine plume dispersion characteristics. The effects of the additional smaller-scale turbulence generated by the down-wind surface roughness are not noticeable even when roughness changes are two orders of magnitude.

6.6 Evaluation of Turbulence Parameterization Schemes

Several first-order turbulence closure schemes and their associated assumptions were compared to wind tunnel data. For example the log velocity profile was not found to exist in the transition region at all; therefore the assumption that local eddy diffusivity varies as $K = \kappa z$ is not acceptable. Similarly, assumptions associated with mixing length theory and $\tau/E = const$ are not valid. On the other hand, mixing assumptions that $K = c_o \kappa z E^{1/2}$ or $(u^2 - w^2)\, dU/dX = 0$ seem justified. Finally, measurements support the conclusion that air flow over a two-dimensional step change of surface roughness preserves two-dimensionality in the turbulence structure; hence, two-dimensional numerical models should be able to simulate the response of mean velocity and turbulence structure to flow over two-dimensional step changes of surface roughness.

7.0 REFERENCES

Briggs, G. (1973), "Diffusion Estimation for Small Emissions," ATDL Contribution File No. 79, Atmospheric Turbulence and Diffusion Laboratory, Oak Ridge, TN.

Cermak, J.E. (1975), "Applications of Fluid Mechanics to Wind Engineering - A Freeman Scholar Lecture", *J. Fluids Eng.*, 97, 9-38.

Counihan, J. (1975), "Adiabatic Atmospheric Boundary Layers: A Review and Analysis of Data from the Period 1880-1972", *Atmos. Environ.*, 9, 871-905.

Elliott, W.P. (1958), "The Growth of the Atmospheric Internal Boundary", *Trans. Am. Geophys. Union*, 39, 1048-1054.

Jackson, P.S. and Hunt, J.C.R. (1975), "Turbulent Wind Flow Over a Low Hill", *Quart J. R. Met. Soc.*, 101, 929-395.

Meroney, R.N. (1981), "Physical Simulation of Dispersion in Complex Terrain and Valley Drainage Flow Situations", *Air Pollution Modelling and Its Application I*, C. De Wispelaere, Ed., Plenum Press, New York, pp. 489-508.

Meroney, R.N. (1990), "Fluid Dynamics of Flow Over Hills and Mountains: Insights Obtained Through Physical Modeling," Chapter 7 of AMS Monograph on *Current Directions in Atmospheric Processes Over Complex Terrain,* AMS Monograph Volume 23, Number 45, June 1990, pp. 145-172.

Panofsky, H.A. and Townsend, A.A.(1964), "Change of Terrain Roughness and the Wind Profile", *Quart. J.R. Met. Soc.*, 86, 390-398.

Snyder, W.H. (1982), "Guidelines for Modeling Atmospheric Diffusion," U.S. Environmental Protection Agency Report EPA-600/8-81-009, Research Triangle Park, NC. 185 pp.

Taylor, P.A. (1967), "On Turbulent Wall Flow Above a Change in Surface roughness", Ph.D. Dissertation, Univ. of Bristol, Canada.

Townsend, A.A. (1961a), "Equilibrium Layers and Wall Turbulence", *J. Fluid Mech.*, 11, 97-120.

Townsend, A.A. (1965b), "Self-preserving Flow Inside a Turbulent Boundary Layer," *J. Fluid Mech.*, 22, 773-797.

Walmsley, J.L., Taylor, P.A. and Keith, T. (1986), "A Simple Model of Neutrally Stratified Boundary-Layer Flow over Complex Terrain with Surface Roughness Modulations", *Boundary Layer Meteorol.*, 36, 157-186.

Wu, G. , Higuchi, K. and Meroney, R.N. (1991), "Applications of Digital Image Processing in Wind Engineering," *8th International Conference on Wind Engineering*, University of Western Ontario, London, Ontario, Canada, 8-12 July, 1991.

Wu, G. (1992), Wind Tunnel Simulation of Turbulence Structure and Dispersion Processes for Air Flow Over a Step Change of Surface Roughness, Ph.D. Dissertation, Civil Engineering, Colorado State University, Fort Collins, 259 pp.

Table 1 Summary of Test Configurations and Surface Characteristics

Case No.	Upstream	Downstream	$(Z_o)_x$ (cm)	n	C_f
	X < 0 cm	X > 100			
1	Smooth	Smooth	0.75	0.12	0.0013
2	Rough	Rough	13.4	0.16	0.0020
3	Very Rough	Very Rough	115.	0.34	0.0040
4	Smooth	Rough			
5	Rough	Smooth			
6	Smooth	Very Rough			
7	Very Rough	Smooth			

Table 2 Comparison of boundary-layer parameters in wind tunnel to atmospheric field values.

Parameter	Case No.	Model	Counihan (1975)	Error (%)
p	1 2 3	0.123 0.16 0.34	0.11 0.17 0.25	-12 3 -27
C_f	1 2 3	0.0013 0.0020 0.0040	0.0015 0.0022 0.0028	11 11 -31
$u'/U_{10\,m}$	1 2 3	0.093 0.204 0.304	0.121 0.185 0.307	30 -9 1
$w'/U_{10\,m}$	1 2 3	0.051 0.106 0.143	0.060 0.093 0.153	18 -13 7
L_{Ux} (m)	1 2 3	41 35 29	150 90 60	**

** Different estimates of integral scales often vary by factors of 2 to 3, but the tendency to reduce values for larger surface roughness is reproduced.

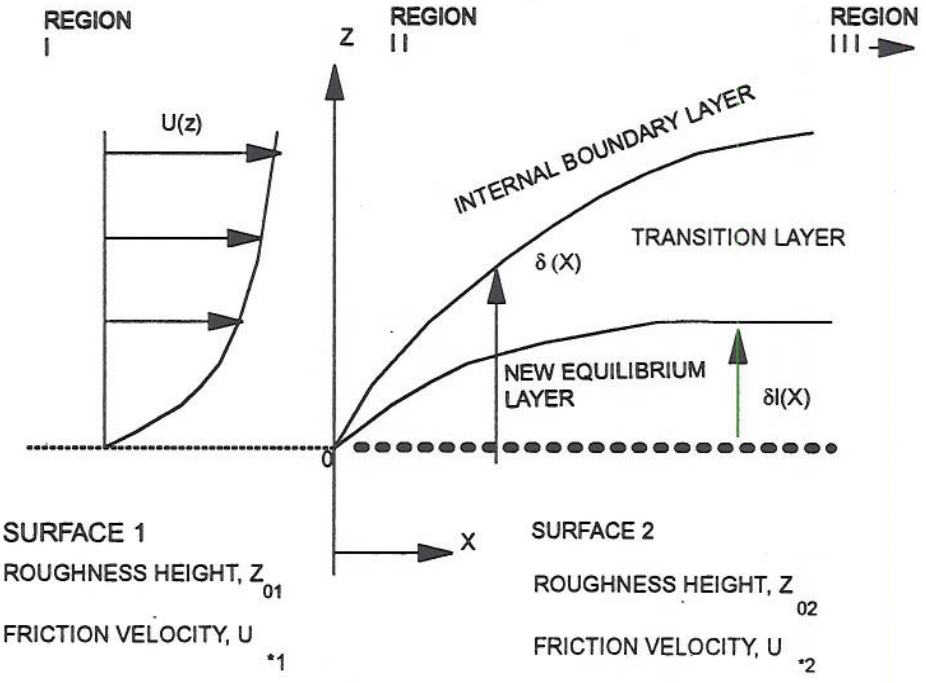

Figure 1 Schematic of flow regions up- and downstream of a transition in surface roughness.

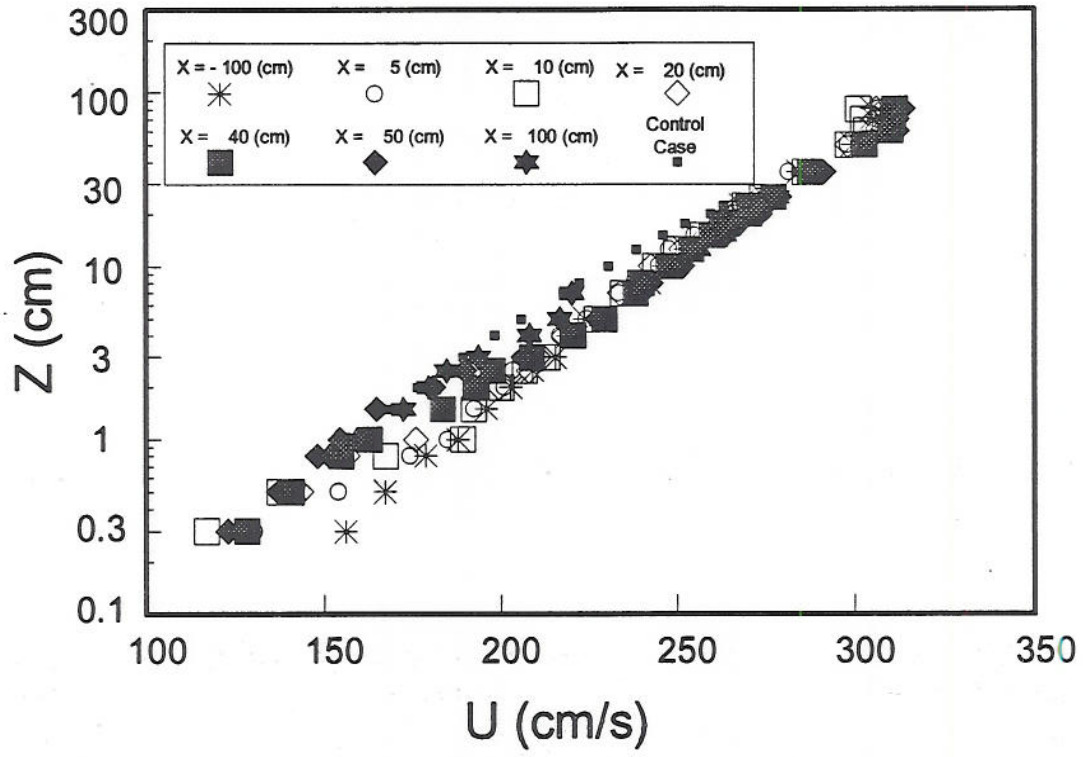

Figure 2 Velocity profiles at wind-tunnel centerline for Case 4: Smooth to rough surface roughness transition.

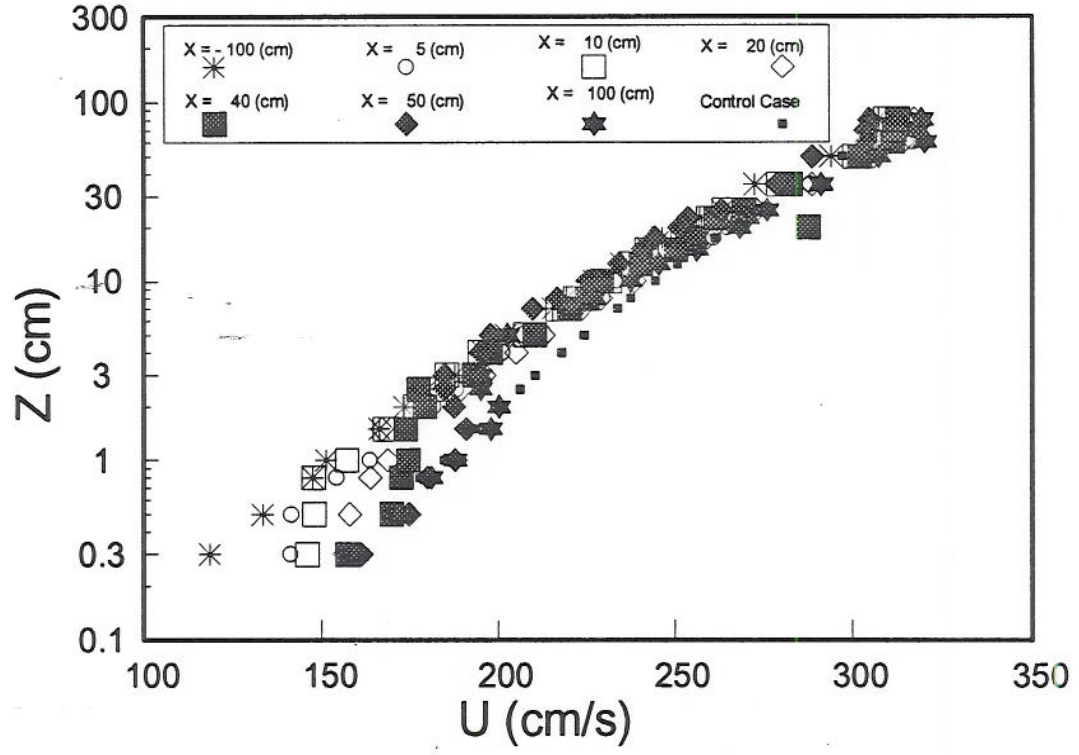

Figure 3 Velocity profiles at wind-tunnel centerline for Case 5: Rough to smooth surface roughness transition.

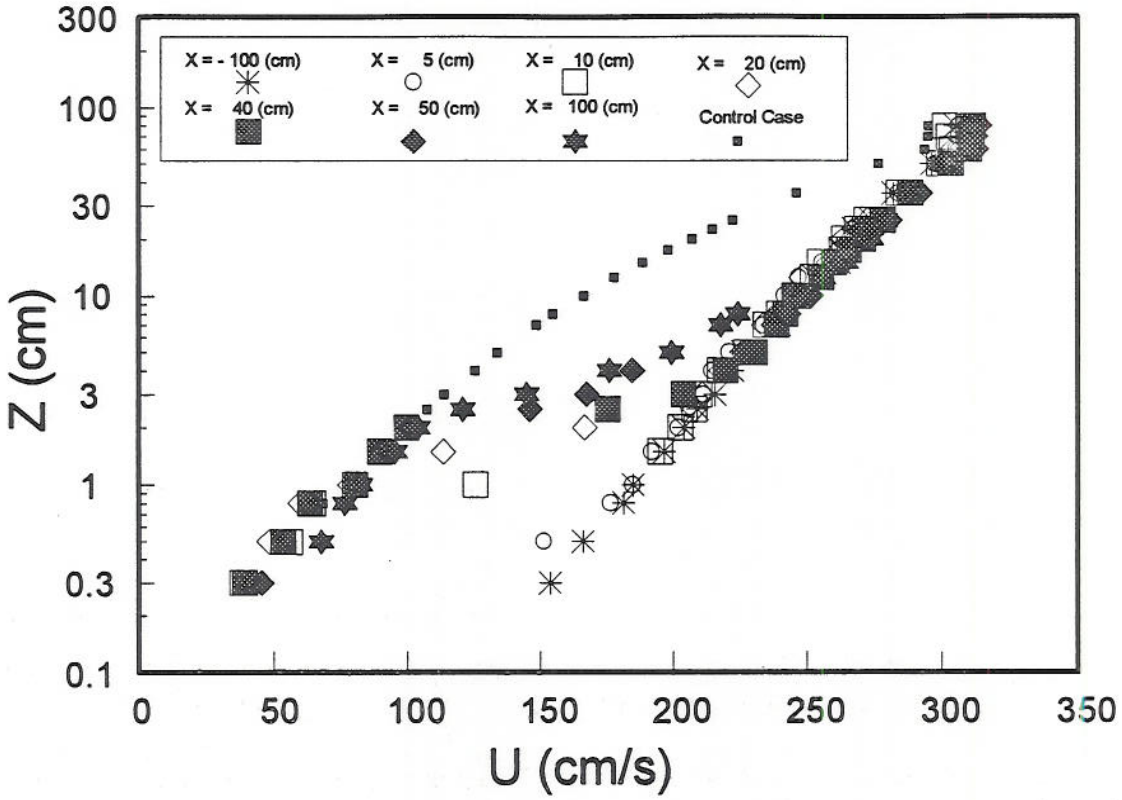

Figure 4 Velocity profiles at wind-tunnel centerline for Case 6: Smooth to very rough surface roughness transition.

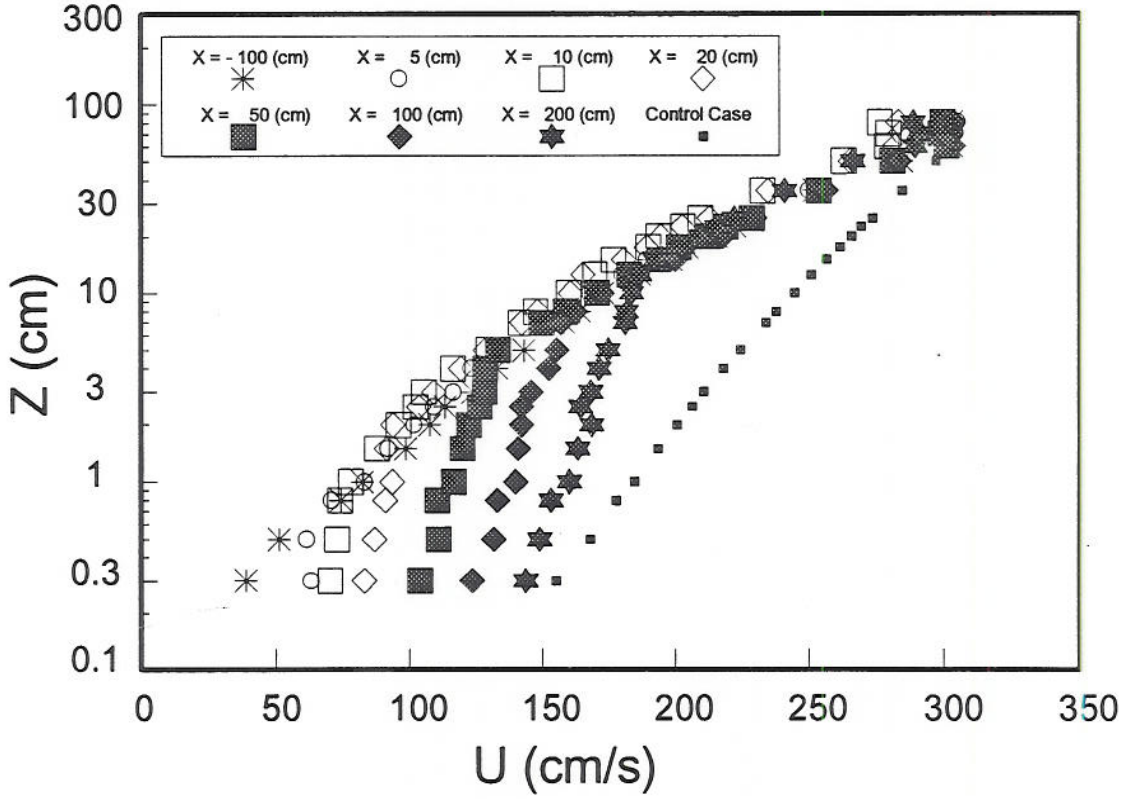

Figure 5 Velocity profiles at wind-tunnel centerline for Case 7: Very rough to smooth surface roughness transition.

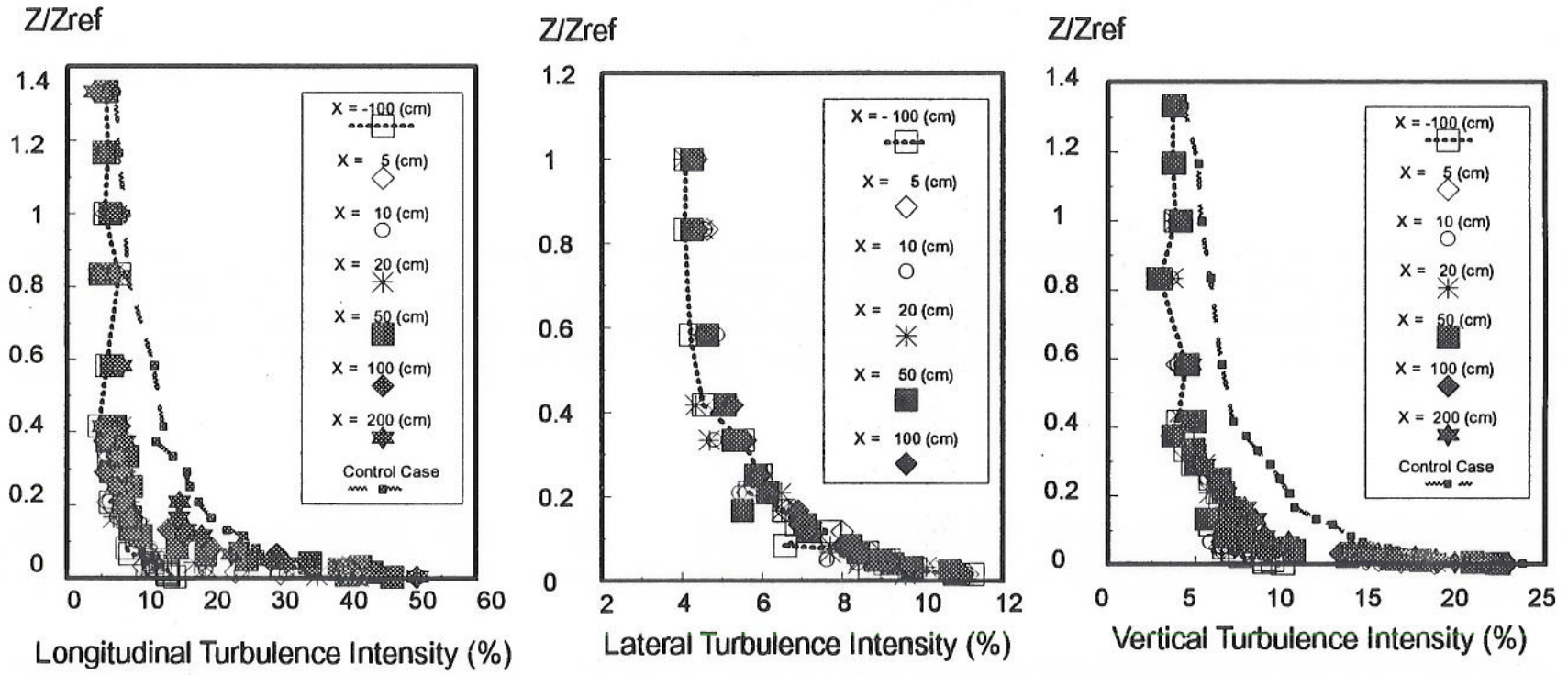

Figure 6 Longitudinal, lateral and vertical turbulence intensity profiles at wind-tunnel centerline for Case 6: Smooth to very rough surface roughness transition.

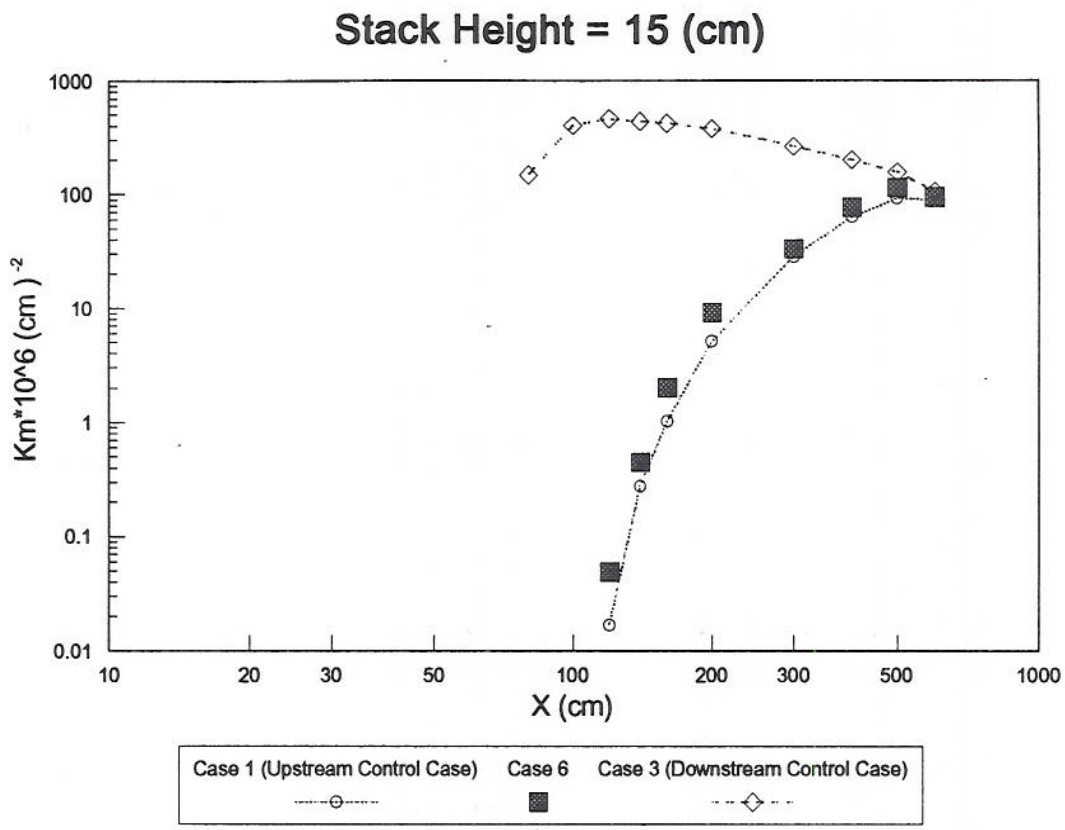

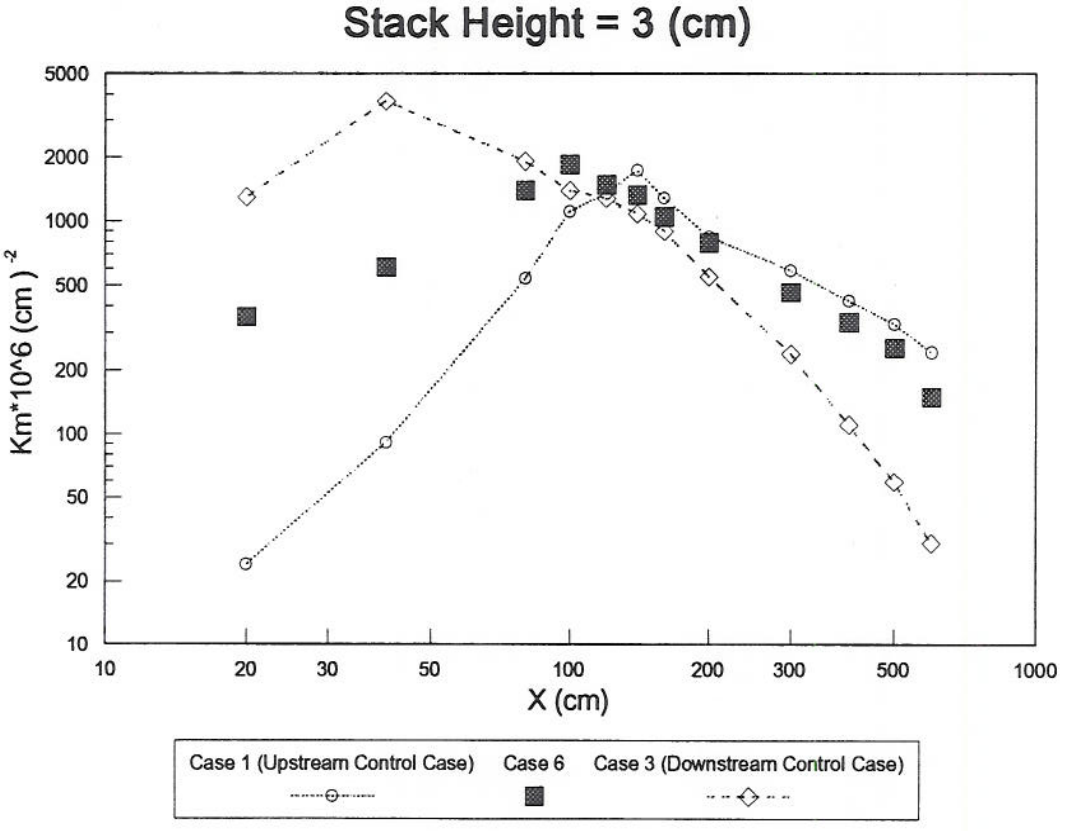

Figure 7 Comparison of ground-level concentrations for high and low stack releases in Cases 1, 6 and 3. Case 1 is smooth, Case 3 is very rough and Case 6 is a smooth to very rough surface roughness transition.

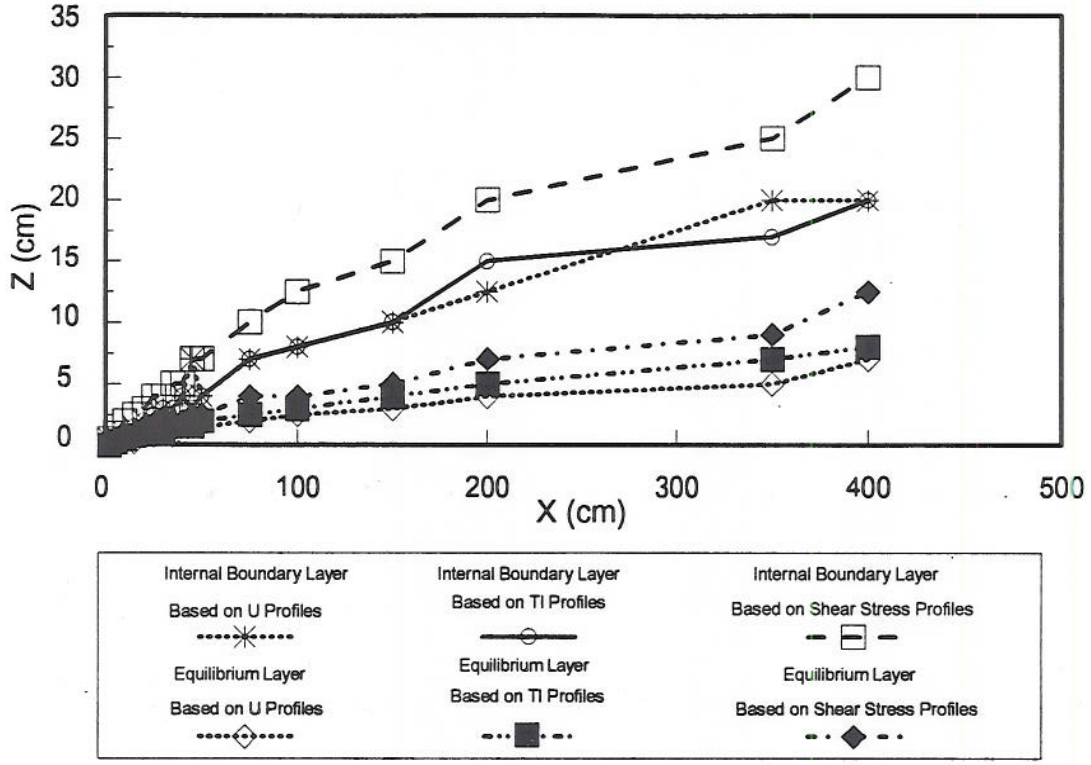

Figure 8 Development of internal boundary layers and equilibrium layers for Case 4: Smooth to rough surface roughness transition.

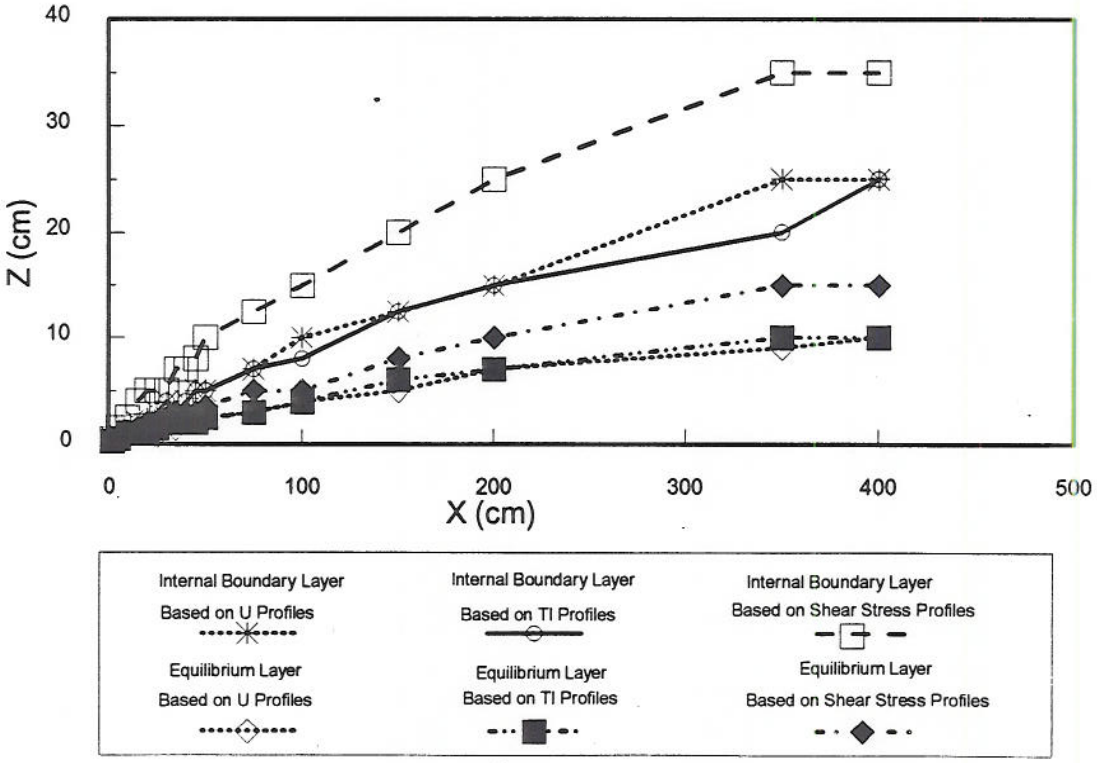

Figure 9 Development of internal boundary layers and equilibrium layers for Case 6: Smooth to very rough surface roughness transition.